Sensor Fault Detection in Building Energy Management Systems

Dionyssia. Kolokotsa[1], Anastasios Pouliezos[2] and George. Stavrakakis[2]

[1]*Technological Educational Institute of Crete*, [2] *Technical University of Crete, tasos@dpem.tuc.gr*

***Abstract*— In this paper a methodology for detecting sensor failures in building energy management systems (BEMS) is presented. The fault diagnosis decision criterion is the average absolute prediction error between the actual and the predicted values of the sensor. The predicted value is calculated by a model based on faultless operation data. Three experiments are presented with simulated biases in the temperature, illuminance and CO_2 sensors. Although the concept is simple, the results for fault detection are quite satisfactory.**

***Index Terms*— Fault detection and diagnosis, sensors, building energy management systems.**

I. INTRODUCTION

Energy is a mainstay of modern industrial society 0. The energy sources on which the European energy infrastructure is based are mostly fossil fuels, namely petroleum,n natural gas and coal. The energy use can be divided into three end use segments: transportation, residential and commercial buildings, and industrial ones. Each of these sectors consumes about one-third of the total energy use. The energy consumption in the building sector represents almost 40% of the total energy consumption in Europe whilst contributing significantly to the greenhouse gas emissions. On the other hand, there is increasing international concern with climate change, and the targets agreed by the European Union under the Kyoto Protocol to reduce emissions of greenhouse gases in 2010 by 8% compared to 1990 levels represent a real challenge 0, 0. The complexity of systems deployed on modern buildings, necessitates the use of optimal control. During the last years, there is a rapid convergence of the technologies of Informatics, Microelectronics and Control Systems leading to novel approaches and solutions for energy and building automation related problems.

As the 'intelligent building' is passing nowadays its phase of maturity, a great number of manufacturers offer integrated solutions (i.e. the ORCA system of Delta Controls based in BACNET architecture, SIEMENS EIB, ABB, etc).

The fault detection and diagnosis (FDD) technology provides the capability to deal with complex problems that are related with the uninterrupted operation of various systems even in a fault regime.

The uninterrupted system operation is based on the normal operation of each of the system parts. In building energy and indoor environment management systems these parts are: (i) sensors, (ii) actuators and (iii) interfaces (wiring) and software.

Sensor information is very important, since its malfunction is amplified through the feedback loop. It is therefore not surprising that a significant effort has been put in designing fault detection and diagnosis subsystems for sensors. Standard methodσ for detecting sensor failures include utilizing the consistency of redundant measurements, estimating expected values from measurements, and intelligent methods (neural nets, fuzzy methods, genetic algorithms).

Fault detection and diagnosis of building HVAC systems usually uses data from sensors to get information on whether the system has faults or not. A Building Energy Management System usually stores the sensors measured data and is accessible from an FDD system. The use of measured data leads to different FDD systems. These can be either knowledge- (0, 0) or model-based (0, 0, 0).

In the present paper a fault detection algorithm is presented for building energy management system sensors built around the SIEMENS EIBUS architecture.

II. PROBLEM STATEMENT

The problem that we are tackling is the detection of sensor failures of the control system depicted in Fig. 1. The equations representing Fig. 1 are:

Nonlinear state equation: $x_{k+1} = f(x_k, u_k, d_k)$

Noisy measurements: $y_k = x_k + n_k$

Fuzzy controller: $u_k = g(r, y_k)$

The state space vector is:

$$x_i = \begin{bmatrix} x_{1,i} & x_{2,i} & x_{3,i} & x_{4,i} & x_{5,i} & x_{6,i} \end{bmatrix}^T = \\ = \begin{bmatrix} T_{in} & T_{mr} & h_{in} & v_{in} & l_{in} & C_{in} \end{bmatrix}^T \quad (1)$$

where

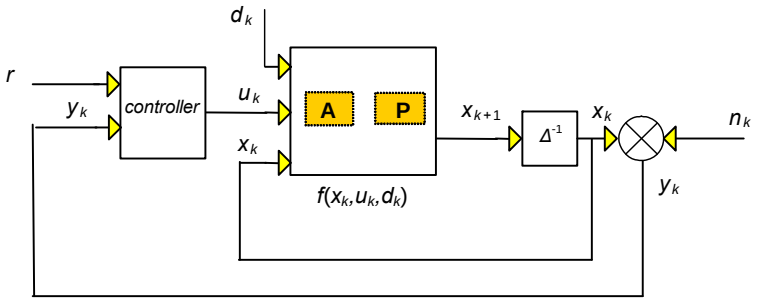

Fig. 1. The control diagram

T_{in} the indoor temperature (°C)
T_{mr} the indoor mean radiant temperature (°C), 0
h_{in} the indoor relative humidity (%)
v_{in} the indoor wind velocity (m/s)
l_{in} the indoor illuminance levels (lux)
C_{in} the indoor CO_2 concentration (ppm)

The measurement vector is,

$$y_i = x_i + n_i$$

where n_i is unknown white noise, and the control vector,

$$u_i = [u_{1,i} \quad u_{2,i} \quad u_{3,i} \quad u_{4,i}]^T = [S \quad W \quad AC \quad L]^T \qquad (2)$$

where

S: the shading opening; 0 (fully shut) to 1 (fully open).
W: the window opening; 0 (fully shut) - 100% (fully open) .
AC: the air conditioning operation duration; -100% (cooling) to +100% (heating) as a percentage of sampling period.
L: the lighting level; 0 (lights off) – 1 (lights fully on).

The disturbances vector consists of (indicative):

t_{out}: the outdoor temperature (°C), measured.
s_d: the number of smoking people.
n_p: the number of occupants.
v_{out}: the outdoor wind velocity.
d_{out}: the outdoor wind direction.
o_d: the opening and closing of doors.
l_{out}:the outdoor illuminance.
h_{out}: the outdoor relative humidity.
t_{app}: the thermal casual gains.
$CO_{2,out}$: outdoor CO_2 concentration.

Finally **A** is the actuators and **P** the overall installation.

I. Modeling and Identification

For each sensor a linear-in-the-parameters, lumped parameter model of the following form is identified:

$$y_p(k) = y_p(k\text{-}1) + \beta_1 f_1(u(k\text{-}1), y_p(k\text{-}1), d(k\text{-}1)) + \ldots + \beta_m \cdot f_m(u(k\text{-}1), y_p(k\text{-}1), d(k\text{-}1)) \qquad (3)$$

where k is the time of sampling, f a non linear function (actually bilinear), u the actuators that influence the value of each specific sensor, y the measured values of the sensors, d the measured values of disturbances and β_i the coefficients that are estimated using a least squares method.

It should be noted that (3) is different for each sensor.

To identify the faultless models, data were sampled at 2 mins. over a 12-hour period (360 samples). The period of experiments was February 2005.

It is important to have an idea of the actuator values during the experiment, so as to judge the identification excitation properties. These are shown in Fig. 2, along with the external temperature plot (remember we are dealing with a scaled plant-booth, inside a laboratory; this explains the rather high values relevant to the season).

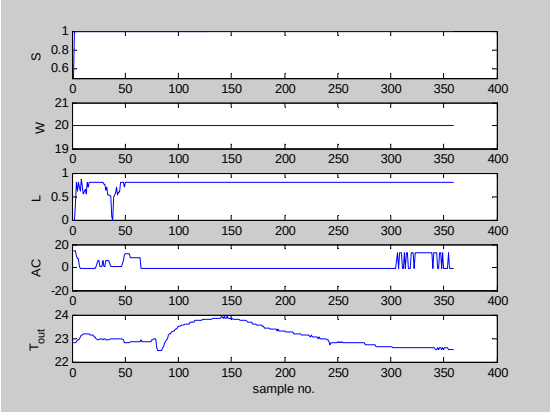

Fig. 2 No fault actuator and external temperature histories

As can be seen, the values for the external shutter (S) and window opening (W) are rather constant. In order to overcome this deficiency, small normal artificial noise was added.

The identification results follow.

A. CO_2 Concentration

The indoor CO_2 concentration at time k is considered a function of the indoor concentration at time k-1, the opening of windows W and the outdoor CO_2 concentration. Since the outdoor CO_2 concentration is not measured in these experiments, it is considered constant. Since outdoor CO_2 concentration remains fairly constant a good fit is expected. Therefore,

$$CO_2(k) = CO_2(k\text{-}1)+\alpha_1 \cdot W(k\text{-}1)[CO_{2,out}\text{-}CO_2(k\text{-}1)]$$
$$= CO_2(k\text{-}1)+\beta_1 \cdot W(k\text{-}1)+\beta_2 \cdot W(k\text{-}1)CO_2(k\text{-}1) \quad (4)$$

where β_1= 0.16, β_2= -0.00039. Fig. 3 shows the good fit of this model on the faultless CO_2 data.

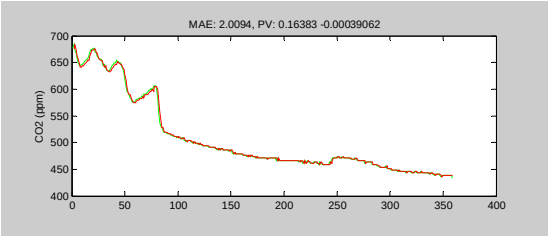

Fig. 3. Actual and predicted CO_2 values on faultless model

B. Illuminance

The indoor illuminance at time k is considered a function of the shading opening S, the indoor electric lighting level L, and the outdoor illuminance (Eq. 5). The outdoor illuminance varies significantly and therefore cannot be considered constant. However it is not measured in the current measurements, and is expected to deteriorate the process performance.

$$Ill_{in}(k) = a_1 \cdot S(k\text{-}1) \cdot Ill_{out} + a_2 \cdot L(k\text{-}1)$$
$$= \beta_1 \cdot S(k\text{-}1) + \beta_2 \cdot L(k\text{-}1) \quad (5)$$

with β_1= 77.66, β_2 = - 43.5. Fig. 4 shows the expected (bad) fit.

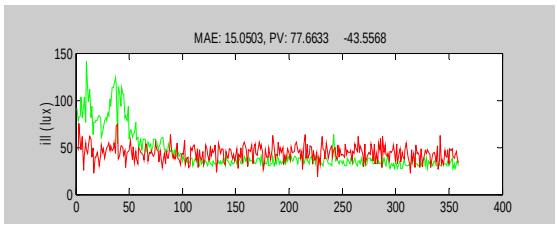

Fig. 4 Actual and predicted indoor illuminance values on faultless model.

C. Temperature

The indoor temperature at time k is considered a function of the indoor temperature at time k-1, the window opening W, the air conditioning level AC and the outdoor temperature T_{out}. Since the outdoor temperature is measured a good fit is expected.

$$T_{in}(k) = T_{in}(k\text{-}1) + \beta_1 \cdot AC(k\text{-}1) + \beta_2 \cdot W(k\text{-}1)[T_{out}(k\text{-}1)\text{-}T_{in}(k\text{-}1)] +$$
$$\beta_3 \cdot [T_{out}(k\text{-}1) - T_{in}(k\text{-}1)]$$
$$= (1\text{-}\beta_3) \cdot T_{in}(k\text{-}1) + \beta_1 \cdot AC(k\text{-}1) + \beta_2 \cdot W(k\text{-}1)[T_{out}(k\text{-}1)\text{-}T_{in}(k\text{-}1)] + \beta_3 \cdot T_{out}(k\text{-}1) \quad (6)$$

where β_1=0.0088, β_2=0.0049, β_3=-0.07. Moreover this equation implies that in the absence of control, the internal temperature approaches the outside at a rate dependent on the building characteristics (expressed by the lumped parameter β_3).

Fig. 5 shows the achieved good fit of this model on the faultless T_{in} data.

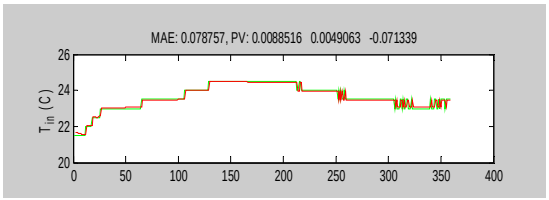

Fig. 5 Actual and predicted indoor temperature values on faultless model.

D. Relative Humidity

The relative humidity at time k is considered a function of the relative humidity at time k-1, the window opening W, the air conditioning level AC and the outdoor relative humidity. Likewise the latter quantity is not measured and is expected to affect the quality of the model, since it is considered constant, although it slowly varies.

$$Hum_{in}(k) = Hum_{in}(k\text{-}1)+a_1 \cdot AC(k\text{-}1)+a_2 \cdot W(k\text{-}1)[Hum_{out}(k\text{-}1)\text{-}Hum_{in}(k\text{-}1)]$$
$$= Hum_{in}(k\text{-}1) + \beta_1 \cdot W(k\text{-}1)+\beta_2 \cdot AC(k\text{-}1)+\beta_3 \cdot W(k\text{-}1)Hum_{in}(k\text{-}1) \quad (7)$$

where β_1= 1.64, β_2= -0.0021, β_2= -0.025. Fig. 6 shows the fit of this model on the faultless relative humidity data.

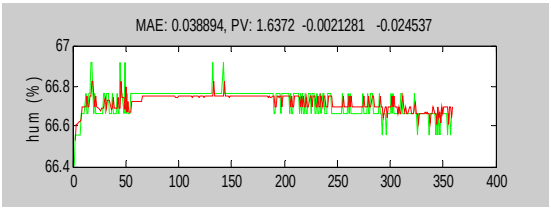

Fig. 6 Actual and predicted indoor relative humidity values on faultless model.

II. Fault Detection

The performance criteria for the fault diagnosis system are the following:

- Capability of detecting multiple faults in different sensors simultaneously.
- Detection speed.
- Number of false alarms or non detection of existing faults (missed detections).
- Size of the detected fault.

The proposed solution utilizes a function $\delta y(k)$ which represents the difference between n the predicted value (y_p) and the actual value (y_r) of each monitored sensor:

$$\delta y(k) = y_p(k) - y_m(k)$$

The decision is based on the mean absolute prediction error (MAPE) defined by the following equation:

$$\varepsilon(k) = \left| \delta y(k) \right| \quad (8)$$

The MAPE is compared to an upper threshold which is calculated by the sample data under normal operation via,

$$\hat{\varepsilon} = \frac{1}{N} \sum_{i=1}^{N} \left| y_p(i) - y_m(i) \right| \quad (9)$$

where N is the sample size.

The methodology used to decide whether a fault exists or

not consists of the following steps:

- At time k the quantity ε_{n_w} is calculated for each sensor by:

$$\varepsilon_{n_w}(k)=\frac{1}{n_w}\sum_{k-n_w+1}^{k}\left|y_p(n_w-i)-y_m(n_w-i)\right|$$

where n_w is the data window length used to robustify the procedure.

- If $\varepsilon_{n_w}(k)>c\cdot\hat{\varepsilon}$ then a fault in the respective sensor is declared, otherwise not. If the fault condition remains for a significant number of samples then the fault certainty increases.

The parameters n_w and c are estimated using trial and error in order for the overall procedure to satisfy the performance criteria. In the specific study n_w=100 and c=2.

III. Experimental Results

The test bench is a scaled plant with the dimensions of a phone booth, especially developed for testing control algorithms in BEMS. It is equipped with the following sensors: (i) temperature (indoor and outdoor), (ii) relative humidity, (iii) CO_2 concentration, (iv) indoor illuminance and (v) indoor wind velocity. It is wired on the Siemens Instabus protocol and interfaced to MATLAB via its OPC server toolbox. It controls automatically its heating and cooling requirements by a small A/C unit, its indoor lighting levels by movable shading devices and artificial lighting and its indoor air quality by movable windows. The control algorithm is a fuzzy rule based on the mean predicted vote (MVP) notion [9].

We performed four experiments (one for each sensor) with a simulated bias of -40% in the corresponding sensor value effected at sample k=20. Sampling was done at 2 mins. and the experiments were run for 12 hours each.

For each sensor the following graphs are produced:

1. The evolution of the decision criterion, i.e. the windowed mean absolute prediction error (WMAPE) together with its upper level for each sensor. This graph shows that a malfunction of a sensor is not mistakenly identified.

2. The evolution of the predicted and actual values.

3. The evolution of the involved actuator values. This is useful for comparison with the identification data and the explanation of possible shortcomings of the detection procedure.

A. Malfunction of indoor temperature sensor

The problem in the operation of the temperature sensor is detected only for the specific sensor as it is shown in Fig. 7 (WMAPE for T_{in} is higher than its upper level). No fault is detected for all the other sensors apart from relative humidity. The reason for the detection of error in the relative humidity sensor is that the relative humidity model is estimated with W equal to 20% (Fig. 2) and the model is "confused" by the 40% window opening that occurs at time k≈180 (Fig. 8). This can be overcome if the learning data are improved.

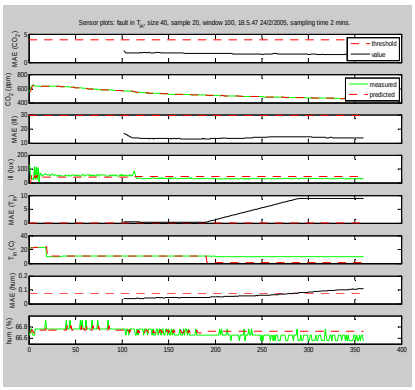

Fig. 7 Sensor and fault criterion plots in the simulated temperature sensor fault

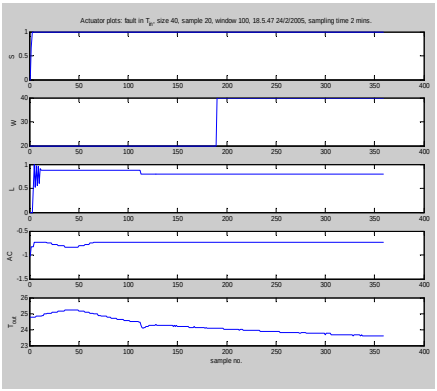

Fig. 8 Actuator plots in the simulated temperature sensor fault

B. Malfunction of illuminance sensor

The malfunction of the indoor illuminance sensor does not cause false alarms for any of the other sensors as depicted in Fig. 9: the WMAPE for illuminance is higher than its upper level indicating the fault of the specific sensor, while all the others are within normal operation limits. This is somewhat surprising given that outdoor illuminance is considered constant in our model.

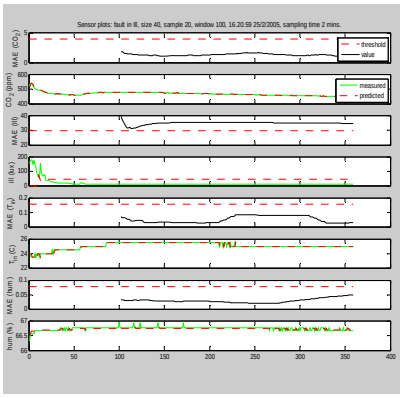

Fig. 9 Sensor and fault criterion plots in the simulated illuminance sensor fault

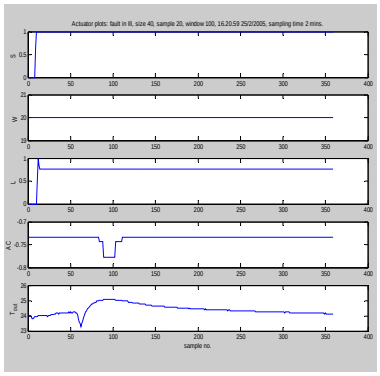

Fig. 10 Actuator plots in the simulated illuminance sensor fault

C. *Malfunction of the CO_2 sensor*

The malfunction of the CO_2 sensor is not detected as depicted in Fig 11. The reason for that is that the relevant actuator values for this sensor are similar both in the normal and faulty case (i.e. 20%, see Fig. 2). This can be predicted mathematically if we consider the relevant equations [10].

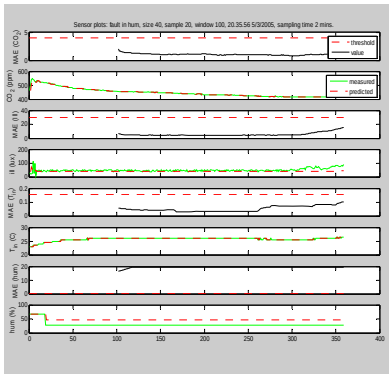

Fig. 11 Sensor and fault criterion plots in the simulated humidity sensor fault

Fig. 12 shows the relevant actuator and external disturbance plots for this experiment.

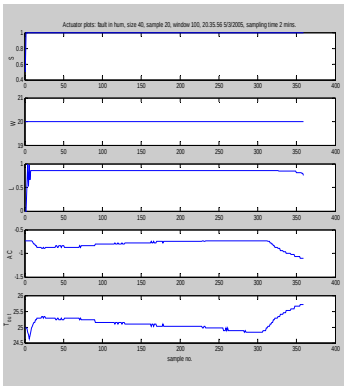

Fig. 12 Actuator plots in the simulated humidity sensor fault

IV. Conclusions

The proposed sensor fault detection system is operating satisfactorily, although it is fairly simple. Some shortcomings can be corrected if the influence of the outside disturbances is minimized. This can be achieved if they can be measured. Further improvements can be effected by a more appropriate training set for each sensor (persistent excitation). Future research will concentrate on carrying over the experiments described here to a real size plant (Laboratory of Industrial Systems at Technical University of Crete).

V. References

[1] F. Kreith and R.E. West, "CRC Handbook on Energy Efficiency", CRC Press, 1997.

[2] ERM Energy, "DGXVII Executive summary: The Dilemma Study". Commission of the European Communities Green Paper, "Towards a European strategy for the security of energy supply", Brussels, 29.11.2000, COM(2000) 769 final.

[3] X. Li, H. Vaezi-Nejad and J.C. Visier, "Development of a Fault Diagnosis Method for Heating Systems Using Neural Networks", *ASHRAE Transactions*, **102 (1),** pp. 607-614, 1996.

[4] J.C. Visier, H. Vaezi-Nejad and P.A. Corrales, "A fault detection tool for school buildings", **105**, Part 1, pp. 543-554, 1999.

[5] S. Kumar, S. Sinha, T. Kojima, T. and H. Yoshida, "Development of parameter based fault detection and diagnosis technique for energy efficient building management system", *Energy Conversion and Management*, **42**, pp.833-854, 2001.

[6] H. Yoshida, S. Kumar, and Y. Morita, "Online fault detection and diagnosis in VAV air handling unit by RARX modeling", *Energy and Buildings*, **33**, pp. 391-401, 2001.

[7] P. Amann, J.M. Perronne, G.L. Gissinger and P.M. Frank, "Identification of fuzzy relational models for fault detection", *Control Engineering Practice*, **9**, pp. 555-562, 2001.

[8] F. Kreider, P. Curtiss and A.Rabl, "Heating and Cooling for buildings: Design for efficiency", McGraw-Hill Higher Education, 2002.

[9] D. Kolokotsa, "Comparison of the performance of fuzzy controllers for the management of the indoor environment", *Building and Environment*, **38**, 12, pp. 1439-1450, 2003.

[10] D. Kolokotsa, A. Pouliezos, G. Stavrakakis, "Sensor fault detection in building energy management systems", Proceedngs, ISKE 2006, Shanghai, China, 6-7 April 2006.